

# Research on infrared image SVM segmentation algorithm for mine drilling and rescue

*In order to identify human body targets and determine miners' locations with infrared images of life information during mine rescue by drilling, the infrared images should be accurately segmented. However, the current segmentation methods fail to meet the requirements due to the inherent limitations and the complex environment of post-disaster roadways. For this, this paper proposes a method of infrared image segmentation based on the SVM (Support Vector Machine) theory. It divides the videos obtained by XKQY-1 infrared life information detectors into positive, negative, and test samples, enhances the infrared images by the top-hat/bot-hat transformation method, adopts the cross validation method to select the optimum parameters  $C$  and  $G$ , trains the data set according to the RBF core function and obtains the SVM classifier to finally achieve the infrared image segmentation of the test samples. After that, this paper compares and analyzes the image segmentation effects with those of the traditional image segmentation methods such as edge detection algorithm, Otsu threshold segmentation method, K-mean clustering method, and morphological watershed method. The results indicate that the SVM-based infrared image segmentation method does not require priori knowledge and pre-processing programs such as the threshold optimization, thus it only takes 0.190s to compute, 24.33% of that in the QGA algorithm; the misclassification error rate is 0.06, 55.05% of that in the QGA algorithm; and the anti-noise capacity is stronger. In a word, this algorithm can be effectively applied in the segmentation of infrared images in mine rescue by drilling and provide great support for subsequent human target identification.*

**Keywords:** Rescue by drilling, life information, infrared image, support vector machine, image segmentation.

## 1. Introduction

In recent years, the number of mine accidents in China has been on a decreasing trend, but the death rate per million tonnes is much higher than that in those coal-producing countries in Europe and the U.S. – many accidents still

happen each year. In some emergency rescue, constrained by some objective conditions like roadway collapses and geological conditions, in order to successfully rescue personnel and protect their lives, ground drilling is the only way, that is, the vertical rescue method. However, the key to vertical rescue is the drilling operations and the search and positioning of the personnel trapped, the latter of which is now a difficult and critical part in vertical mine rescue. For example, during the gypsum mine rescue in Pingyi, Shandong in December 2015, Professor Wen Hu, Deputy Director of State Mine Emergency Rescue (Xi'an) Research Center, used the drilling rescue life information detector developed by his team, which effectively solved the difficult problems like drilling fault detection, trapped personnel search and roadway environmental information and helped successfully rescue a number of trapped miners. Therefore, efficient and accurate drilling life information detection technology plays an important role in the field of mine drilling rescue.

At present, the drilling life information detection visualization devices are designed based on visible light imaging. Affected by light intensity, the effective detection distance is only 15m, but the infrared thermal imaging life information detection technology based on temperature can make up for this shortcoming. Body temperature, as an objective reflection of the intrinsic activities in a human body, is one of the effective means to detect the location and living state of the trapped personnel. As the infrared thermal imager has many advantages like high thermal sensitivity (0.1℃), strong “penetrating” capacity (penetrating through water mist, dark night, smoke and a certain amount of coal dust) and long-range non-contact imaging, etc., many scholars at home and abroad have applied this technology in life information detection, and achieved good results[1-3]. The emergency rescue team from School of Safety Science and Engineering, Xi'an University of Science and Technology has developed an infrared thermal imaging life information detection system for mine rescue by drilling. This system can provide clear imaging of underground roadways and detect the downhole disaster conditions and the status of trapped personnel in real time.

However, in order to enable the system to automatically recognize and warn about human body targets, the infrared

Messrs. Fei Jinbiao, Wen Hu and Zhang Duo, School of Safety Science and Engineering, Xi'an University of Science and Technology, Xi'an 710 054 and also with Xi'an Research Center National Mine Rescue, Xi'an 710 054, China. E-mail:18192066689@163.com

images detected by the system must be segmented accurately. So far, scholars at home and abroad have developed hundreds of image segmentation methods, such as: edge detection method (Sobel, Perwitt and Roberts gradient operator; LoG operator; Canny operator) [4-5], Hough transform method, Otsu threshold segmentation method [6-7] and K-mean clustering method. They have also studied various new infrared image segmentation algorithms based on morphology[9], fuzzy mathematics[10], genetic algorithm [11-12] and neural network[13].

Constrained by the infrared imaging principle, unlike other images, infrared images have low contrast between the target and the environment, blurred edges of targets and great noise. Therefore, it is a great challenge to segment the infrared targets accurately in a complex post-disaster roadway environment. Regarding the blurred edges of targets, scholars proposed the fuzzy clustering method[14] and the fuzzy connectedness algorithm[15], which have effectively reduced the signal-to-noise ratio and can divide the target fuzzy edges clearly, but the computation time is too long and thus they are not suitable for image libraries with larger data sets; Bo[16] et al. proposed the information entropy algorithm to effectively address the blurred target edges in infrared images, but there still existed local segmentation optimization problem; Chittajallu[17] et al. proposed the concept of fuzzy image segmentation, but the positioning of the target edges was not accurate because it did not consider the degree of closeness to the grey level; Liu Songtao[18] et al. used the Gaussian theory to establish the grey scale probability distribution model for the targets and the environment to estimate the likelihood energy of the image segmentation energy function, but as the algorithm converges to the likelihood estimation, it can only achieve local optimum and the whole image segmentation precision is not high. Li[19] et al. introduces the entropy algorithm to realize the automatic segmentation of images with enhanced anti-noise capacity and improved image segmentation precision. Since the energy function of the algorithm is based on the parameter likelihood energy, there is still a problem with the segmentation effect.

Support Vector Machine (SVM) has a strong self-learning ability and follows the principle of structural risk minimization, which solves the problems of over-training and over-fitting in the artificial neural network, and thus has excellent generalization performance[20]. At present, scholars have successfully applied the SVM algorithm in medical, aerial and remote sensing image segmentation[21]. However, the application of SVM is seldom reported in the infrared image segmentation in mine rescues. In order to realize effective segmentation of infrared images in the complex environment of the post-disaster roadways, this paper proposes a new algorithm for infrared image segmentation based on SVM for mine rescue by drilling.

## 2. SVM algorithm

The basic idea of the SVM algorithm is to use the kernel function to map the sample to a certain high-dimensional space so that the linearly inseparable problem in the original low-dimensional space becomes linearly separable.

### 2.1 INTERVAL FUNCTION

Given a training sample set  $(x_i, y_i)$ , where,  $x \in R^N$ ,  $y \in [-1, 1]$ ,  $i = 1, 2, \dots, n$ , there exists an optimal hyper-plane  $\psi$  that accurately splits the target and the environment into two classes:

$$\psi : \vec{\omega} \cdot x_i + b = 0 \quad \dots \quad (1)$$

Let the interval function from  $\vec{x}_i$  to the plane  $\psi$  be:

$$\gamma_i = y_i (\vec{\omega} \cdot x_i + b) \quad \dots \quad (2)$$

where:  $y_i$  is the class label. When it is -1, it indicates a negative sample, when it is 1, it indicates a positive sample.

As the distance from the sample  $\vec{x}_i$  to the plane  $\psi$  is

$\left| \frac{\vec{\omega} \cdot x_i + b}{\|\vec{\omega}\|} \right|$ , we substitute it into formula (2) and obtain:

$$\gamma_i = y_i \left( \frac{\vec{\omega}}{\|\vec{\omega}\|} \right)^T \cdot \vec{x}_i + \frac{b}{\|\vec{\omega}\|} \quad \dots \quad (3)$$

### 2.2 SVM CLASSIFIER

According to formula (3), given the optimal hyper-plane  $\psi$ , the problem is to solve the extreme value of  $\gamma_i$ . The formal expression is as follows:

$$\begin{aligned} \max_{\gamma, \omega, b} : & \frac{\gamma}{\|\vec{\omega}\|} \\ \text{s.t.} : & y_i (\vec{\omega} \cdot x_i + b) \geq \gamma, i = 1, 2, \dots, n \end{aligned} \quad \dots \quad (4)$$

Normalize the global function intervals and then formula (4) is transformed to:

$$\begin{aligned} \min_{\gamma, \omega, b} : & \frac{1}{2} \|\vec{\omega}\|^2 \\ \text{s.t.} : & y_i (\vec{\omega} \cdot x_i + b) \geq 1, i = 1, 2, \dots, n \end{aligned} \quad \dots \quad (5)$$

Multiply the constraint condition in formula (5) by the Lagrange multiplier  $\alpha_i$ , and substitute it into the objective function in formula (5), and then the problem is converted to an unconstrained optimization problem, i.e. the minimization of  $L$  with respect to  $\vec{\omega}$ ,  $b$  and  $\alpha_i$ .

$$\begin{aligned} L(\vec{\omega}, b, \alpha) &= \frac{1}{2} \|\vec{\omega}\|^2 - \sum_{i=1}^n \alpha_i [y_i (\vec{\omega} \cdot x_i + b) - 1] \\ &= \frac{1}{2} \vec{\omega} \cdot \vec{\omega} - \sum_{i=1}^n \alpha_i y_i \vec{\omega} \cdot x_i - \sum_{i=1}^n \alpha_i y_i b + \sum_{i=1}^n \alpha_i \end{aligned}$$

$$\begin{aligned}
&= -\frac{1}{2} \sum_{i=1}^n \sum_{j=1}^n \alpha_i y_i \vec{x}_i^T \alpha_j y_j \vec{x}_j - b \sum_{i=1}^n \alpha_i y_i + \sum_{i=1}^n \alpha_i \\
&= \sum_{i=1}^n \alpha_i - \frac{1}{2} \sum_{i=1}^n \sum_{j=1}^n \alpha_i \alpha_j y_i y_j \vec{x}_i^T \vec{x}_j
\end{aligned}$$

By then, the formula is unrelated to  $\vec{\omega}$  and  $b$ . It is just a function of  $\alpha_i$ . So the optimization problem becomes:

$$\begin{aligned}
\min_{\alpha} : L(\alpha) &= \sum_{i=1}^n \alpha_i - \frac{1}{2} \sum_{i=1}^n \sum_{j=1}^n \alpha_i \alpha_j y_i y_j \vec{x}_i^T \vec{x}_j \\
s.t. : &\begin{cases} \sum_{i=1}^n \alpha_i y_i = 0 \\ 0 \leq \alpha_i \leq \beta \end{cases} \quad \dots (6)
\end{aligned}$$

where,  $\beta$  is the penalty factor.

After  $\alpha$  is solved,  $\vec{\omega}$  and  $b$  can be determined according to the solution  $\alpha$  to the dual problem as follows:

$$\begin{cases} \vec{\omega} = \sum_{i=1}^n \alpha_i y_i \vec{x}_i \\ b = -(\min_{y_i=1}(\vec{\omega} \cdot \vec{x}_i) + \max_{y_i=-1}(\vec{\omega} \cdot \vec{x}_i)) / 2 \end{cases} \quad \dots (7)$$

After the optimal solutions  $\alpha^*$ ,  $\vec{\omega}^*$  and  $b^*$  corresponding to  $\alpha$ ,  $\vec{\omega}$  and  $b$  are solved, the optimal classification function can be obtained as follows:

$$h(\vec{x}) = \text{sgn}(\sum_{i=1}^n \alpha_i^* y_i (\vec{x}_i \cdot \vec{x}) + b^*) \quad \dots (8)$$

where,  $\vec{x}_i$  is the test sample.

### 3. Materials and method

#### 3.1 TEST EQUIPMENT

The experiment used the XKQY-□ infrared life information detector for mine rescue by drilling developed independently by Xi'an University of Science and Technology (as shown in Fig.1), with a pixel resolution of 320×240.

The life information drilling detection system consists of four parts: a borehole life detector (including one circuit for infrared thermal imaging camera, one for visible light imaging, two for audio and one for environmental parameters), high-intensity transmission cables, a ground two-way radio signal transmission control wheel and a special laptop for the system.

The intrusion-type infrared thermal imager automatically captures infrared images of underground accident scenes and sends the collected images, ambient gas parameters and audio signals to the COFDM wireless transmission module. The video and audio synthesis and compression module first converts the analog video and audio signals into digital signals, and then processes them through the H.264 compression coding, QPSK modulation and convolutional



Fig.1 Infrared life information detector

encoding and transmits them to the COFDM transmission module for data transmission at the radio frequency. The ground receiving base station integrates the COFDM data receiving module and radio frequency receiving module, which connect to the computer through USB interfaces. Another redundant design is that the system uses the XDSL network protocol, and improves its intrinsic safety by increasing the maximum transmission distance between the sending and the receiving models to 4Km. The multimedia information collected by the acquisition module is modulated and transmitted to the XDSL module, and then transmitted to the ground through the mine twisted pair. The XDSL module at the ground receiving base station re-modulates the telephone signals into network signals. The XDSL line access module encoder provides an RJ45 client interface, through which, the video and audio information are transmitted and displayed on the computer to the rescue personnel.

#### 3.2 CONDITIONS

Layout information about the device and the operator is shown in Fig.2. The computer configuration includes Intel (R) Core (TM) i7-2600CPU @ 3.40GHz, 8G memory, Win7 (32-bit) system and MATLAB2014a simulation software.

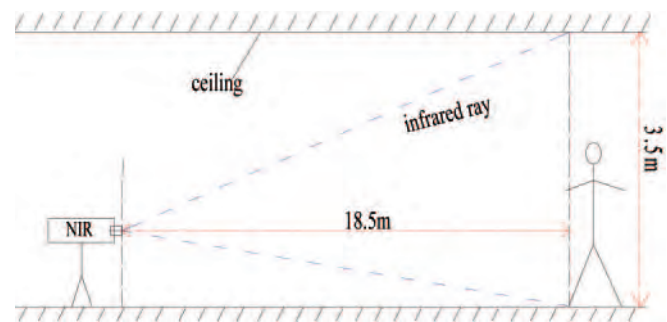


Fig.2 Sketch of the shooting scene



Fig.3 Picture of the roadway used in mine work safety simulation experiment

The essence of image segmentation is to classify the pixels of the image, that is, to distinguish between the pixels of the target and the environment. Each pixel has its corresponding data. In MATLAB2014a, with the use of the SVM algorithm, the segmentation of infrared images can be achieved.

The samples required for the experiment were taken in the mine work safety simulation test roadway, which is shown in Fig.3. During calculation, a  $7 \times 7$  sliding window and the RBF kernel function were selected, and the cross validation method was used to select the best penalty factor and the kernel parameter  $G$ .

### 3.3 IMAGE ENHANCEMENT

In order to optimize the segmentation effect, first of all, the top/bottom cap transformation was conducted to the images[7] and the grey scale contrast was strengthened. In this paper, the radius of the disk structure used for image manipulation is set to be 15 pixels and the enhanced images are shown in Fig.4.

## 4. Experimental result analysis and evaluation

### 4.1 ANALYSIS OF SIMULATION RESULTS

This paper chooses three infrared images for the simulation test, where one person stands upright, one person squats down a little bit and two persons stand, respectively (Fig.3(d)). The infrared images were segmented by the edge detection operator, K clustering (K-mean) method, P

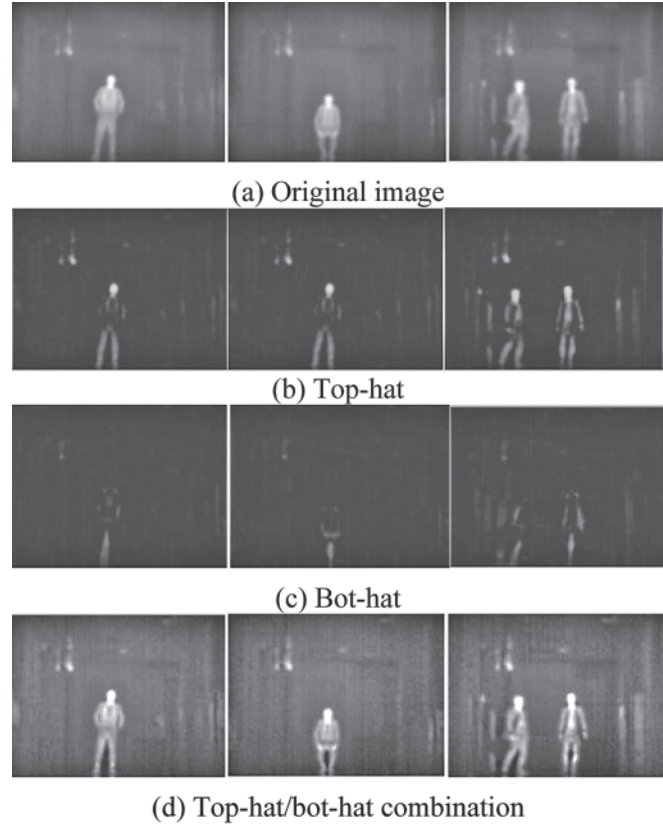


Fig.4 Infrared enhanced effect charts

parameter method (P-tile), watershed algorithm (watershed), Ostu algorithm and the quantum genetic algorithm (QGA) and the results were compared to those by the SVM algorithm. The simulation results are shown in Fig.5 and Fig.6

It can be seen from Fig.4 that the Canny operator and the Log operator did not cut off important information but were affected greatly by noise, and the smoothing effect of the Log operator was not as good as that of the Canny operator. Since both the Sobel operator and the Prewitt operator detect the grey scales of the four adjacent points of the pixel, the results were similar. Comparatively, the Sobel operator has a better anti-noise capacity, but the computation amount is large and the edges are blurred. The Roberts operator detected the difference between the gradients of two adjacent pixels on the diagonal, so the edges were the clearest.

Compared to Fig.5, the target edges in Fig.6 are more continuous and clearer, and affected less by the noise, so the segmentation effect is obviously better than that of the edge detection operator. As shown in Fig.6(a), the K-mean algorithm has poor effect in segmenting the infrared images, because the optimization result of this algorithm in the middle grey center is relatively too high; the P-tile algorithm requires the proportion of the target in the image stay around a certain value so as to effectively separate the target and the environment. In actual practice, the proportion fluctuates with the changes in the environment and the detection distance, so in Fig.6(b), there

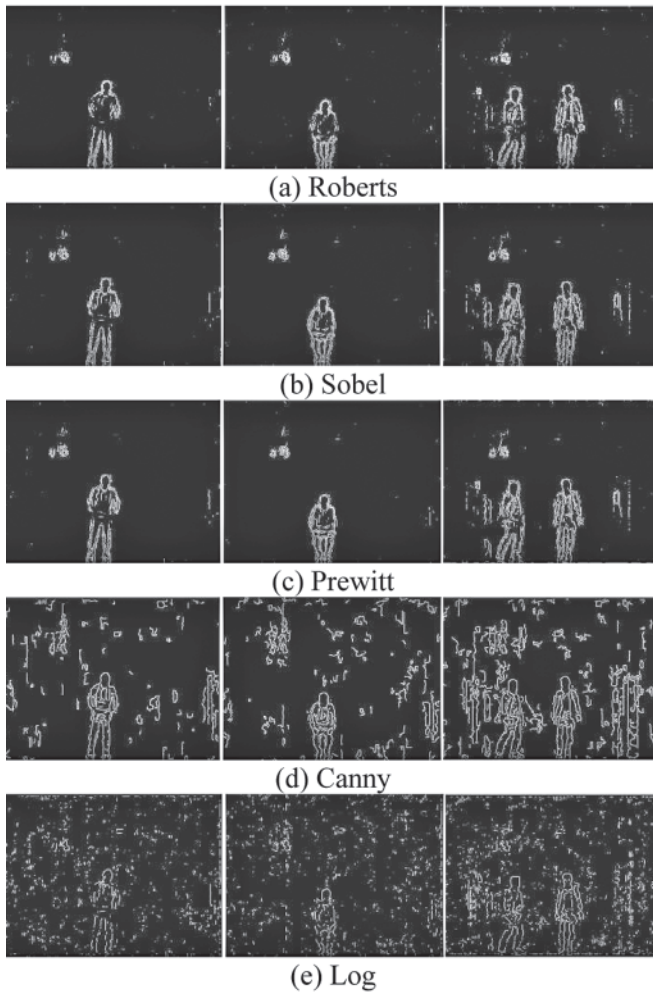


Fig.5 Segmentation effect of the edge detection operator

are some over segmentations. As the Watershed algorithm is highly sensitive to the grey scale variation, it is easily affected by ambient noise, as shown in the two-person image in Fig.6(c). The histogram of an infrared image often has multiple peaks, so the Ostu algorithm, which looks for two peaks to segment the target and the environment is not applicable to infrared images - for example, the segment effect in Fig.6(d) is poor. In Fig.6(e), the segmentation effect of the QGA algorithm is improved compared to those of previous algorithms, but it has fuzzy edge recognition of the target and it does not have a strong noise processing capacity. The SVM algorithm completely separates out the target with a high anti-noise capacity and gives clear target edges, so the segmentation effect is the best.

In order to compare the anti-noise performance of each algorithm, impulse noise was added to the image where a person stands upright before it was segmented. The result is shown in Fig.7

It can be seen from Fig.7 that under the severe interference of impulse noise, the SVM algorithm can still completely separate out the human target, while the segmentation effect of the QGA algorithm becomes much poorer.

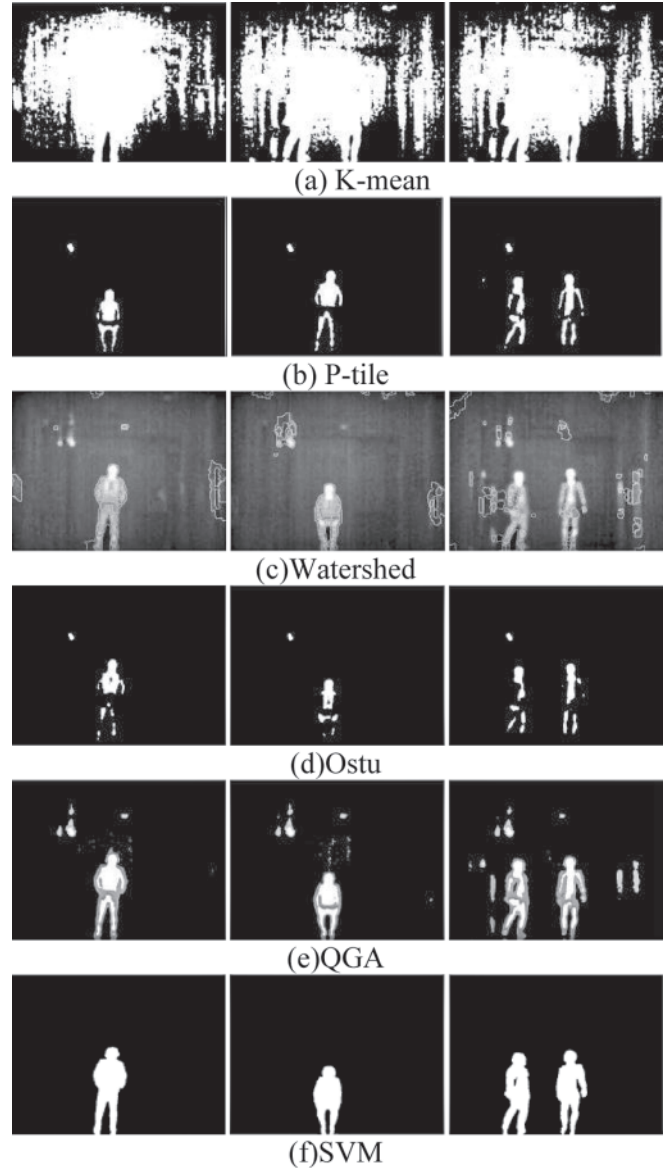


Fig.6 Segmentation effects of different infrared image segmentation algorithms

#### 4.2 EFFECT EVALUATION

To objectively evaluate the segmentation performance, this paper compares the segmentation time and classification error (ME) rates of various algorithms by taking the segmentation of the image where a person stands upright as an example[22]

(1) Time comparison (Table 1)

(2) ME comparison

According to the literature [22], the smaller the ME, the better is the image segmentation effect. The formula is as follows:

$$ME = 1 - \frac{|B_0 \cap B_\gamma| + |F_0 \cap F_\gamma|}{|B_0| + |F_0|} \quad \dots \quad (9)$$

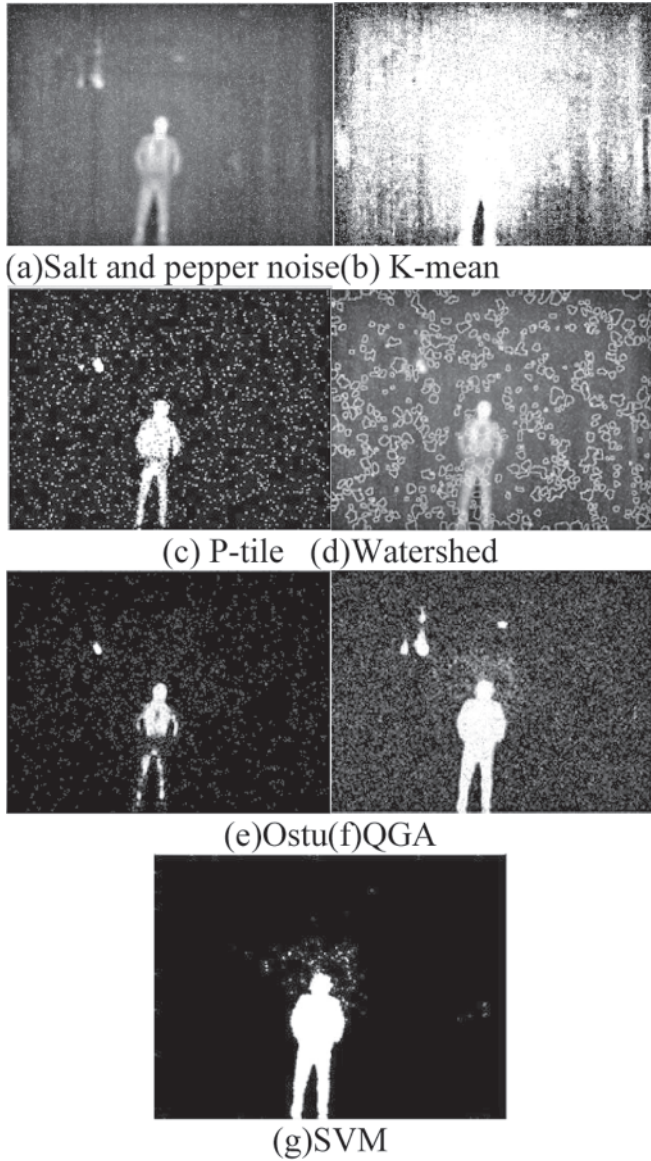


Fig.7 Comparison of the anti-noise performances

where,  $B_0$  is the sum of the background pixels in the ideal segmentation of the image;  $B_y$  is the sum of the background pixels in the algorithm simulation result;  $F_0$  is the sum of the target pixels in the ideal segmentation; and  $F_y$  is sum of the target pixels in the algorithm simulation result.

The ME values of various algorithms in segmentation of the image are calculated according to formula (9) (Fig.8). It can be seen from Table 1 and Fig.8 that both the run time and the misclassification error rate of the SVM algorithm are low, among which, the run time accounts for only 24% of that by the QGA algorithm. As the SVM algorithm uses the trained

TABLE I: CALCULATION TIME OF EACH ALGORITHM

Algorithm	K-mean	P-tile	Watershed	Ostu	QGA	SVM
Time/s	2.189	3.101	2.824	3.037	0.781	0.190

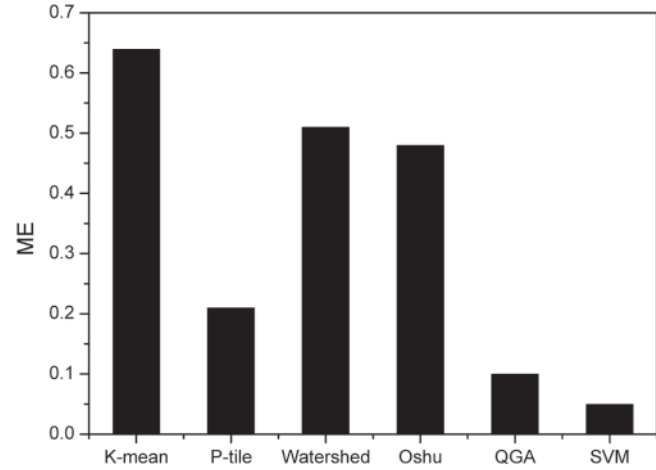


Fig.8 Misclassification rate comparison chart

classifier, it saves the trouble of determining parameters like threshold, membership function, and middle grey center.

## 5. Conclusions

Through comparison of various infrared image segmentation algorithms, it is found that the SVM segmentation algorithm has the best infrared image segmentation effects. It only takes 0.190s to compute, accounting for 24.33% of that in the QGA algorithm; the ME rate is 0.06, 55.05% of that in the QGA algorithm; and the anti-noise capacity is stronger.

The SVM infrared image segmentation algorithm can be effectively applied in the life information detection system for mine rescue by drilling to provide scientific support for the real-time monitoring on the disaster and incident development trend and give timely and accurate data support for the search and positioning of the personnel trapped during vertical rescue.

## References

- Chen, J. M. and Liang, D. C. (2009): "Application of infrared LED in temperature monitoring system," *Electric Power Automation Equipment*, Vol. 29, No. 5, pp.139-141, 2009.
- Jiang, G. , Zhang, F. G. and Fan, Y. F. (2010): "Fault analysis of 110 kV substation PT," *Electric Power Automation Equipment*, Vol. 30, No.10, pp. 139-140+144, 2010.
- Yang, B. D. and Li, L. (2007): "Influence factors of relative temperature difference determination method of infrared diagnosis for electrical equipment," *Laser and Infrared*, Vol. 7, No. 4, pp. 341-343, 2007.
- Zouagui, T., Benoit-Cattin, H. and Odet, C. (2004): "Image segmentation functional model," *Pattern Recognition*, Vol. 37, No. 9, pp. 1785-1795, 2004.
- Madabhushi, A. and Metaxas, D. N. (2003): "Combining low-

- high-level and empirical domain knowledge for automated segmentation of ultrasonic breast lesions,” *IEEE Trans Med Imaging*, Vol. 22, No. 2, pp. 155-169, 2003.
6. Otsu, N. (1979): “A threshold selection method from a gray level histograms,” *IEEE Transactions Systems, SMC-9*, pp. 62-66, 1979.
  7. Men, H., Yu, J. X. and Qin, L. (2011): “Segmentation of electric equipment infrared image based on CA and OTSU,” *Electric Power Automation Equipment*, Vol. 31, No. 9, pp. 92-95, 2011.
  8. Yun, T. J., Guo, Y. C. and Gao, C. (2008): “Human Segmentation Algorithm in Infrared Images Based on K-means Clustering Centers Analysis,” *Opto-Electronic Engineering*, Vol. 35, No. 3, pp. 140-144, 2008.
  9. Chen, X. M., Ni, G. Q. and Liu, M. Q. (2001): “On Infrared Image Segmentation Algorithm Based on Watershed,” *Journal of Optoelectronics Laser*, Vol. 12, No. 10, pp. 1072-1075, 2001.
  10. Yin, S. B., Wang, Y. B. and Deng, Z. (2016): “Infrared image segmentation based on graph cut of fast recursive fuzzy 2-partition entropy,” *Optics and Precision Engineering*, Vol. 24, No. 3, pp. 668-680, 2016.
  11. Qu, S. R. and Yang, H. H. (2015): “Infrared image segmentation based on PCNN with genetic algorithm parameter optimization,” *High Power Laser and Particle Beams*, Vol. 27, No. 5, pp. 051007(1-6), 2015.
  12. Zhang, S. S., Gu, Y. F. and Zhang, J. P. (2007): “A method of infrared image segmentation based on quantum genetic algorithm,” *Journal of Harbin Institute of Technology*, Vol. 39, No. 9, pp. 1427-1430, 2007.
  13. Hu, C. Y., Zhao, B. J. and He, P. K. (2007): “IR image segmentation method based on fractal theory and neural network,” *Systems Engineering and Electronics*, Vol. 29, No. 5, pp. 720-722, 2007.
  14. Liu, G., Liang, X. P. and Zhang, J. G. (2011): “Contourlet transform and improved fuzzy c-means clustering based infrared image segmentation,” *Systems Engineering and Electronics*, Vol. 33, No. 2, pp. 443-448, 2011.
  15. Ciesielski, K. C., Herman, G. T. and Kong, T. Y. (2015): “General theory of fuzzy connectedness segmentations,” *Neurocomputing*, Vol. 24, No. 6, pp. 170-186, 2015.
  16. Bo, H., Ma, F. L. and Han, B. J. (2005): “SAR image segmentation based on immune algorithm,” Proceedings of the Fifth International Conference on Control and Automation, Shanghai, P.R. China, ICCA, pp. 1279-1282, 2005.
  17. Chittajallu, D. R., Brunner, G. and Kurkure, U. (2009): “Fuzzy-cuts: A knowledge-driven graph-based method for medical image segmentation,” 2009 IEEE Conference on Computer Vision and Pattern Recognition (CVPR), Alaska, US: IEEE, pp. 715-722, 2009.
  18. Liu, S. T., Wang, H. L. and Yin, F. L. (2012): “Interactive ship infrared image segmentation method based on graph cut and fuzzy connectedness,” *Acta Automatica Sinica*, Vol. 38, No. 11, pp. 1735-1750, (in Chinese), 2012.
  19. Li, Y., Mao, X., Feng, D. and Zhang, Y. N. (2011): “Fast and accuracy extraction of infrared target based on Markov random field,” *Signal Processing*, Vol. 91, No. 5, pp. 1216-1223, 2011.
  20. Vapnik, V. N. (1995): “The Nature of Statistical Learning Theory, New York,” NY: Springer-Verlag, 1995.
  21. Xu, S. P. (2008): “Survey of Study on Image Segmentation Based on SVM,” University of Science and Technology Liaoning, pp. 40-52, 2008.
  22. Zhou, D. G., Gao, C. and Guo, Y. C. (2013): “Simplified Pulse Coupled Neural Network with Adaptive Multilevel Threshold for Infrared Human Image Segmentation,” *Journal of Computer-Aided Design and Computer Graphics*, Vol. 25, No. 2, pp. 208-214, 2013.

## Journal of Mines, Metals & Fuels

*Special issue on*

# CONCLAVE I ON EXPLOSIVES

*Price per copy Rs. 200; GBP 20.00 or USD 40.00*

*For copies please contact :*

The Manager, Books & Journals Private Ltd, 6/2 Madan Street, Kolkata 700 072

Tel.: 0091 33 22126526; Fax: 0091 33 22126348; e-mail: bnjournals@gmail.com